Photon statistics of pulse-pumped four-wave mixing in fiber with weak signal injection*

Nan-Nan Liu(刘楠楠), Yu-Hong Liu(刘宇宏), Jia-Min Li(李嘉敏), and Xiao-Ying Li(李小英)†

College of Precision Instrument and Opto-electronics Engineering, Tianjin University, Key Laboratory of Optoelectronics Information Technology of Ministry of Education, Tianjin 300072, China

(Received 16 January 2016; published online 30 May 2016)

We study the photon statistics of pulse-pumped four-wave mixing in fibers with weak coherent signal injection by measuring the intensity correlation functions of individual signal and idler fields. The experimental results show that the intensity correlation function of individual signal (idler) field $g^{(2)}_{s(i)}$ decreases with the intensity of signal injection. After applying narrow band filter in signal (idler) band, the value of $g^{(2)}_{s(i)}$ decreases from 1.9 ± 0.02 (1.9 ± 0.02) to 1.03 ± 0.02 (1.05 ± 0.02) when the intensity of signal injection varies from 0 to 120 photons/pulse. The results indicate that the photon statistics changes from Bose–Einstein distribution to Poisson distribution. We calculate the intensity correlation functions by using the multi-mode theory of four-wave mixing in fibers. The theoretical curves well fit the experimental results. Our investigation will be useful for mitigating the crosstalk between quantum and classical channels in a dense wavelength division multiplexing network.

Keywords: photon statistics, four-wave mixing, intensity correlation function, fiber optics

PACS: 42.50.–p, 42.50.Dv, 42.65.–k, 03.67.Hk **DOI:** 10.1088/1674-1056/25/7/074203

1. Introduction

Pulse-pumped four-wave mixing (FWM) in $\chi^{(3)}$ optical fibers is not only a powerful tool to realize optical amplification in broadband and flexible wavelength range,[1] but also an efficient method for generating quantum lights which can be used to fulfill different kinds of quantum information processing schemes.[2–4] So far, the spontaneous four-wave mixing (SFWM) realized by launching only the pump fields into fibers and FWM realized by launching both coherent signal injection (with photon number $|\alpha|^2 \gg 1$) and pump fields into fibers have been extensively investigated. The former has been exploited to generate entangled photon pairs and squeezed state;[5–10] the latter has been exploited to realize all optical function generation for classical fiber optical communication[1] and to generate squeezed state for quantum information processing.[11–13] However, the pulse-pumped FWM with signal injection of a few photons is less studied.

On the other hand, for practical quantum communication, quantum signal carried by entangled photon pairs must be integrated into the existing fiber network. Since the optical power used for classical channels is many orders of magnitude higher than that for quantum channels, the optical nonlinear effects such as FWM and spectral broadening induced by self-phase modulation and Raman scattering may lead to additional noise for quantum communication.[14–17] Therefore, the investigation about FWM with weak signal injection will help figure out the solution for mitigating nonlinear effect induced impairment on the quantum channels.

Photon statistics is often exploited to characterize the properties of an optical field.[18,19] For a quasi continuos wave pumped FWM in fiber with weak signal injection, Voss *et al.* reported the measurement of the photon number distribution of signal field by using optical homodyne tomography (OHT).[20] For a pulse-pumped FWM with weak signal injection, however, it is challenging to study the photon statistics by OHT, because the mode matching required by the OHT is difficult to realized owning to the multi-mode nature of signal and idler fields.[21] In this paper, we will study the photon statistics by measuring the intensity correlation functions of individual signal and idler fields with a Hanbury Brown–Twiss (HBT) interferometer, which has been used to successfully characterize the photon statistics of the multi-mode signal and idler fields generated by the pulse-pumped SFWM.[22,23]

The rest of the paper is organized as follows. In Section 2, we describe the experimental setup of pulse-pumped FWM in fiber. In Section 3, we present our experimental results of intensity correlation function obtained by varying the intensity of signal injection and analyze the data by using the multi-mode theory of FWM. The theoretical analysis well explains the experimental results. Finally, we end with a brief summary and discussion in Section 4.

*Project supported by the National Natural Science Foundation of China (Grant No. 11527808), the State Key Development Program for Basic Research of China (Grant No. 2014CB340103), the Specialized Research Fund for the Doctoral Program of Higher Education of China (Grant No. 20120032110055), the Natural Science Foundation of Tianjin, China (Grant No. 14JCQNJC02300), the Program for Changjiang Scholars and Innovative Research Team in University, China, and the Program of Introducing Talents of Discipline to Universities, China (Grant No. B07014).

†Corresponding author. E-mail: xiaoyingli@tju.edu.cn

© 2016 Chinese Physical Society and IOP Publishing Ltd

2. Experiment

Our experimental setup is shown in Fig. 1. FWM is taken place in 300-m dispersion shift fiber (DSF). The 90/10 fiber coupler (FC1) is used to couple 10% of the signal injection and 90% of the pump fields into the DSF. The DSF is submerged in liquid nitrogen (77 K) for suppressing Raman scattering. The nonlinear coefficient, zero dispersion wavelength, and dispersion slope of the DSF are about 2 W^{-1}/km, 1548 nm, and 0.081 $ps{\cdot}nm^{-2}{\cdot}km^{-1}$, respectively.

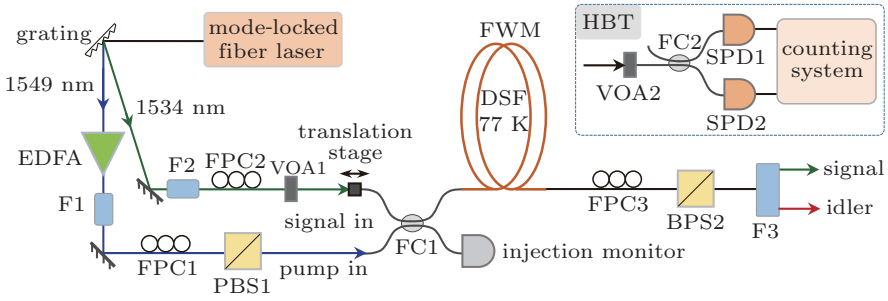


Fig. 1. (color online) Experimental setup. DSF: dispersion shift fiber; EDFA: erbium-doped fiber amplifier; F1–F3: filters; FC1: 90/10 fiber coupler; FC2: 50/50 fiber coupler; FPC1 and FPC3: fiber polarization controllers; HBT: Hanbury Brown–Twiss interferometer; PBS1 and PBS2: polarization beam splitters; VOA1 and VOA2: variable optical attenuators; SPD1 and SPD2: single photon detectors.

To obtain the pump and signal injection of the FWM, we first disperse the 36-MHz train of 100-fs pulses centered at 1550 nm from a mode-locked fiber laser with a grating and then spectrally filtering them to obtain two synchronous beams with central wavelengths of about 1549 nm and 1534 nm, respectively. Under this condition, the co-polarized FWM with a broad gain bandwidth is phase matched.[24] The signal injection centering at 1534 nm can be significantly amplified by co-propagating with the pump through the DSF and the idler beam centering at 1564.3 nm will be created at the output of DSF. The signal injection field is propagated through the 1534-nm channel of the arrayed waveguide grating filter (F2) with full width at half maximum (FWHM) of about 0.38 nm to further suppress the noise photons leaked through the grating. To adjust the photon number of signal injection, the output of F2 is attenuated by a variable optical attenuator (VOA1). To achieve the required pump power, we then feed the pump pulses into an erbium-doped fiber amplifier (EDFA). The output of the EDFA is further cleaned up with a bandpass filter F1 having central wavelength and FWHM of about 1549 nm and 0.8 nm, respectively. The power of the pump are controlled by a fiber polarization controller (FPC1) and a fiber polarization beam splitter (PBS1).

For the realization of maximized FWM gain in fiber, it is important to match the modes of the pump and the signal injection. To do so, we send the output of the DSF into an optical spectrum analyzer (not shown in Fig. 1) for monitoring the spectrum of FWM. The relative time delay between the signal injection and the pump is optimized by a translation stage placed at the "signal in" port (see Fig. 1). The polarization mode is matched by using the FPC2. Figure 2 shows the spectrum of the FWM with maximized gain when the photon number of signal injection and the average pump power are about 30 photons/pulse and 0.6 mW, respectively. As a comparison, the spectrum of the signal injection is plotted in the inset of Fig. 2, which is obtained by blocking the pump input.

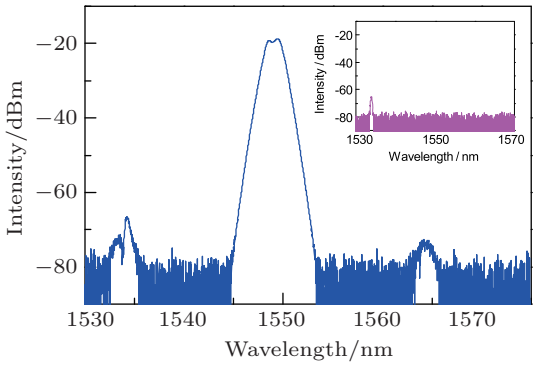


Fig. 2. (color online) Spectrum of the optimized FWM for coherent signal injection with intensity of about 30 photons/pulse. The inset is the spectrum of the signal injection.

The amplified signal and idler fields co-polarized with the pump are selected by adjusting FPC3 placed in front of PBS2. The dual-band filter F3, whose central wavelengths in the signal and idler bands are about 1534 nm and 1564.3 nm, respectively, is used to suppress the pump field and to separate signal and idler fields. The pump-rejection ratio of F3, realized by cascading two coarse wavelength division multiplexing (CWDM) filters with a wave shaper (Finisar Waveshaper 4000S), is in excess of 120 dB. The FWHM of F3 in both signal and idler bands is about 0.4 nm.

We characterize the photon statistics by launching individual signal/idler field into a HBT interferometer and measuring the normalized intensity correlation function $g_s^{(2)}/g_i^{(2)}$. Since the value of $g^{(2)}$ is independent upon the transmission and detection efficiency,[22,25] we heavily attenuate the amplified signal/idler field to single photon level by using the

VOA2. In the HBT interferometer, the attenuated signal/idler field is fed to the input port of the 50/50 fiber coupler (FC2), and the two outputs of FC2 are detected by single photon detectors (SPD, id200) SPD1 and SPD2, respectively. The two SPDs are operated in the gated Geiger mode. The 2.5-ns gate pulses of SPDs arrive at a rate of about 3.6 MHz, which is 1/10 of the repetition rate of the pump pulses, and the dead time of the gate is set to be 10 μs.

3. Results and analysis

During the measurement of $g^{(2)}_{\mathrm{s(i)}}$, the average pump power is fixed at 0.6 mW. For a given intensity of signal injection, we record both the coincidence and accidental coincidence rates of two SPDs by detecting signal (idler) fields originated from the same and adjacent pump pulses, respectively.[22] The normalized intensity correlation function $g^{(2)}_{\mathrm{s(i)}}$ is the ratio between the measured coincidence and accidental coincidence rates. Figure 3 shows the measured $g^{(2)}_{\mathrm{s}}$ (circles) and $g^{(2)}_{\mathrm{i}}$ (diamonds), obtained by varying the intensity of signal injection (in the unit of photons per pulse). One sees that both the $g^{(2)}_{\mathrm{s}}$ and $g^{(2)}_{\mathrm{i}}$ are about 1.9 when the photon number of signal injection is 0, which is close to the single mode nature of the thermal field ($g^{(2)}=2$). This is because the narrow band filter F3 is applied at the output of the DSF.[22,23] However, with the increase of intensity of signal injection, $g^{(2)}_{\mathrm{s(i)}}$ decreases quickly. When the injection photon number is larger than 100, both $g^{(2)}_{\mathrm{s}}$ and $g^{(2)}_{\mathrm{i}}$ approach to 1. We notice that, for a fixed intensity of signal injection, $g^{(2)}_{\mathrm{s}}$ is always slightly smaller than $g^{(2)}_{\mathrm{i}}$.

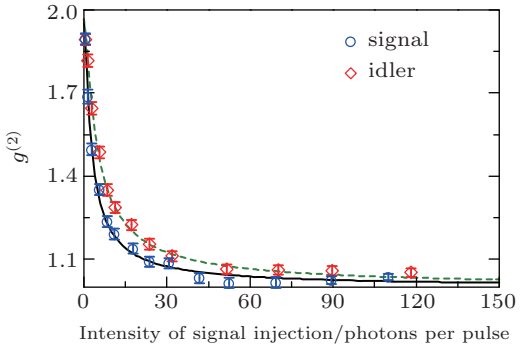


Fig. 3. (color online) The intensity correlation functions $g^{(2)}$ of signal (circles) and idler (diamonds) fields. The solid and dash curves are the theoretical fits of the $g^{(2)}_{\mathrm{s}}$ and $g^{(2)}_{\mathrm{i}}$, respectively.

To explain the experimental results in Fig. 3, we theoretically analyze the dependence of $g^{(2)}_{\mathrm{s}}$ and $g^{(2)}_{\mathrm{i}}$ according to the multi-mode theory of pulse-pumped FWM in fiber.[24] Since the dispersion slope of the DSF is very small and the central wavelength of the Gaussian shaped pump is in the anomalous-dispersion regime, we assume the phase matching condition of the FWM is perfect. In this case, $g^{(2)}_{\mathrm{s(i)}}$ can be calculated and expressed as (see Appendix A for detailed derivation)

$$g^{(2)}_{\mathrm{s(i)}}=1+\frac{2H^{\mathrm{st}}_{\mathrm{s(i)}}+H^{\mathrm{sp}}_{\mathrm{s(i)}}}{(I^{\mathrm{st}}_{\mathrm{s(i)}}+I^{\mathrm{sp}}_{\mathrm{s(i)}})^2}, \tag{1}$$

with

$$H^{\mathrm{st}}_{\mathrm{s}}=|\alpha|^2\sum_{n_1,n_2,n_3,n_4=0}^{\infty}\frac{|G|^{2n_1+2n_2+2n_3+2n_4+2}}{(2n_1)!(2n_2+1)!(2n_3)!(2n_4+1)!}\frac{\sqrt{2}\sigma\sigma_{\mathrm{s}}^2}{\sqrt{16x_{\mathrm{s}}y_{\mathrm{s}}z_{\mathrm{s}}+4(x_{\mathrm{s}}y_{\mathrm{s}}+2(x_{\mathrm{s}}+y_{\mathrm{s}})z_{\mathrm{s}})\sigma_{\mathrm{s}}^2+(x_{\mathrm{s}}+y_{\mathrm{s}}+4z_{\mathrm{s}})\sigma_{\mathrm{s}}^4}}, \tag{2}$$

$$H^{\mathrm{st}}_{\mathrm{i}}=|\alpha|^2\sum_{n_1,n_2,n_3,n_4=0}^{\infty}\frac{|G|^{2n_1+2n_2+2n_3+2n_4+4}}{(2n_1+1)!(2n_2+1)!(2n_3+1)!(2n_4+1)!}\frac{\sqrt{2}\sigma\sigma_{\mathrm{i}}^2}{\sqrt{16x_{\mathrm{i}}y_{\mathrm{i}}z_{\mathrm{i}}+4(x_{\mathrm{i}}y_{\mathrm{i}}+2(x_{\mathrm{i}}+y_{\mathrm{i}})z_{\mathrm{i}})\sigma_{\mathrm{i}}^2+(x_{\mathrm{i}}+y_{\mathrm{i}}+4z_{\mathrm{i}})\sigma_{\mathrm{i}}^4}}, \tag{3}$$

$$H^{\mathrm{sp}}_{\mathrm{s(i)}}=\sum_{n_1,n_2,n_3,n_4=0}^{\infty}\frac{|G|^{2n_1+2n_2+2n_3+2n_4+4}}{(2n_1+1)!(2n_2+1)!(2n_3+1)!(2n_4+1)!}\times\frac{\sigma_{\mathrm{s(i)}}^2}{4\sigma_{\mathrm{p}}\sqrt{(2+n_1+n_2+n_3+n_4)\sigma_{\mathrm{s(i)}}^2+4(1+n_1+n_3)(1+n_2+n_4)\sigma_{\mathrm{p}}^2}}, \tag{4}$$

$$I^{\mathrm{st}}_{\mathrm{s}}=|\alpha|^2\sum_{n_1,n_2=0}^{\infty}\frac{|G|^{2n_1+2n_2}}{(2n_1)!(2n_2)!}\frac{\sigma\sigma_{\mathrm{s}}}{\sqrt{\sigma^4+\sigma^2\sigma_{\mathrm{s}}^2+2\sigma_{\mathrm{p}}^2((n_1+n_2)(2\sigma^2+\sigma_{\mathrm{s}}^2)+8n_1n_2\sigma_{\mathrm{p}}^2)}}, \tag{5}$$

$$I^{\mathrm{st}}_{\mathrm{i}}=|\alpha|^2\sum_{n_1,n_2=0}^{\infty}\frac{|G|^{2n_1+2n_2+2}}{(2n_1+1)!(2n_2+1)!}\frac{\sigma\sigma_{\mathrm{i}}}{\sqrt{\sigma^4+\sigma^2\sigma_{\mathrm{i}}^2+2\sigma_{\mathrm{p}}^2((1+n_1+n_2)(2\sigma^2+\sigma_{\mathrm{i}}^2)+2(1+2n_1)(1+2n_2)\sigma_{\mathrm{p}}^2)}}, \tag{6}$$

$$I^{\mathrm{sp}}_{\mathrm{s(i)}}=\sum_{n_1,n_2=0}^{\infty}\frac{|G|^{2n_1+2n_2+2}}{(2n_1+1)!(2n_2+1)!}\frac{\sigma_{\mathrm{s(i)}}}{2\sigma_{\mathrm{p}}\sqrt{2(1+n_1+n_2)}}, \tag{7}$$

where $G\propto\gamma P_{\mathrm{p}}L$ is the gain coefficient of FWM; $|\alpha|^2$ (in the unit of photons/pulse) is the photon number of the signal injection (see Eq. (A5) in Appendix A); σ, σ_{p}, and $\sigma_{\mathrm{s(i)}}$ are the bandwidths of the signal injection, pump field, and F3, respectively. For clarity, we use the coefficients $x_{\mathrm{s}}=\sigma^2+4n_2\sigma_{\mathrm{p}}^2$, $y_{\mathrm{s}}=\sigma^2+4n_4\sigma_{\mathrm{p}}^2$, $x_{\mathrm{i}}=\sigma^2+2(1+2n_2)\sigma_{\mathrm{p}}^2$, $y_{\mathrm{i}}=$

$\sigma^2+2(1+2n_4)\sigma_p^2$, $z_s=z_i=(1+n_1+n_3)\sigma_p^2$ in Eqs. (2) and (3).

In Eq. (1), the term $H_{s(i)}$ represents the second-order correlation of the amplified signal (idler) field, while the term $I_{s(i)}$ represents the intensity of the amplified signal (idler) field. From Eqs. (2)–(7), one sees that the terms labeled with superscript sp, $H^{sp}_{s(i)}$ and $I^{sp}_{s(i)}$, are independent upon the signal injection with intensity $|\alpha|^2$, which means they are contributed by spontaneous emission of FWM in DSF; while the terms labeled with superscript st, $H^{st}_{s(i)}$ and $I^{st}_{s(i)}$, are proportional to $|\alpha|^2$, which means that they are contributed by stimulated emission of FWM in DSF. When the intensity of signal injection is $|\alpha|^2=0$, the FWM is so called spontaneous four-wave mixing (SFWM). In this case, $g^2_{s(i)}$ is related to the gain coefficient G and the ratio between the bandwidth of the filter and that of the pump $\sigma_{s(i)}/\sigma_p$, which has been studied in detail.[22,23] When the intensity of signal injection is very high, the amplified signal (idler) field originated from stimulated emission dominates. In this case, the terms contributed by the spontaneous emission in Eq. (1) can be ignored and the correlation function can be simplified as $g^2_{s(i)}\approx 1+2H^{st}_{s(i)}/(I^{st}_{s(i)})^2\approx 1+|\alpha|^2/|\alpha|^4\approx 1$. When the intensity of signal injection is very weak, the amplified signal (idler) field is the sum of the photons originated from stimulated and the spontaneous emissions, i.e., all the terms $H^{st}_{s(i)}$, $H^{sp}_{s(i)}$, $I^{st}_{s(i)}$, $I^{sp}_{s(i)}$ in Eq. (1) contribute to $g^2_{s(i)}$. When the gain coefficient G and the bandwidths σ, $\sigma_{s(i)}$, σ_p are fixed, the values of $H^{st}_{s(i)}/|\alpha|^2$, $H^{sp}_{s(i)}$, $I^{st}_{s(i)}/|\alpha|^2$, $I^{sp}_{s(i)}$ are constants (see Eqs. (2)–(7)). In this situation, the contribution of the stimulated terms increases with the intensity of signal injection $|\alpha|^2$, and the value of $g^2_{s(i)}$ decreases with $|\alpha|^2$. In addition, for a fixed intensity of signal injection $|\alpha|^2$, the proportion of spontaneous photons in amplified signal field is smaller than that in amplified idler field. The relation is not obvious in Eqs. (5) and (6), but is straightforward to deduce by exploiting a single mode theory.[24] Therefore, the $g^{(2)}_s$ is always slightly smaller than $g^{(2)}_i$ for a fixed $|\alpha|^2$.

To quantitatively understand the experimental results, we first fit the experimental data $g^{(2)}_s$ in Fig. 3 by substituting the experimental parameters $\sigma=0.38$ nm, $\sigma_s=\sigma_i=0.4$ nm, $\sigma_p=0.8$ nm and $|\alpha|^2$ into Eqs. (1)–(7) and by varying the coefficient G. We find the optimized fitting is obtained for $G=2.5$. We then substitute the experimental parameters and $G=2.5$ into Eqs. (1)–(7), and plot the theoretical curves of $g^{(2)}_s$ (solid curve) and $g^{(2)}_i$ (dash curve) in Fig. 3. The results indicate that the theoretical curves well fit the experimental data.

4. Discussion and summary

In summary, we investigated the photon statistics of the pulse-pumped FWM with weak coherent signal injection by measuring the normalized intensity correlation functions of individual signal and idler fields. The measured photon statistics is a combination effect of the stimulated emission of signal injection and the spontaneous emission originated from vacuum. In particular, when narrow band filter is applied in signal (idler) field, the measured normalized intensity correlation function $g^{(2)}_{s(i)}$ decreases from 1.9 ± 0.02 (1.9 ± 0.02) to 1.03 ± 0.02 (1.05 ± 0.02) with the intensity of signal injection varies from 0 photons/pulse to 120 photons/pulse. The results indicate that the photon statistics of individual signal and idler fields change from Bose–Einstein distribution to Poisson distribution. We also theoretically analyze the dependence of $g^{(2)}_s$ and $g^{(2)}_i$. The calculated results well fit the experimental data. Our investigation not only helps to deepen the understanding of the photon statistics of FWM in fibers but also is useful for studying the crosstalk between the classical and quantum channels in a dense wavelength division multiplexing network for quantum communication.[14,16]

It is worth pointing out that our weak signal injection is in the coherent state. However, for quantum communication exploiting the existing dense wavelength division multiplexing network, the additional noise photons in quantum channels may originated from Raman scattering of classical signal,[14,17] which is in the multi-mode thermal state. For a more complete understanding of FWM in fiber, it is necessary to further study the photon statistics by using the thermal state as an injection of FWM.

Appendix A: Derivation of the intensity correlation function

According to the multi-mode theory of pulse-pumped FWM in fiber,[24] we start our derivation of the intensity correlation functions of individual signal and idler fields from the input–output relation

$$\hat{b}_s(\omega_s)=\int_S h_{1s}(\omega_s,\omega_s')\hat{a}_s(\omega_s')\,\mathrm{d}\omega_s' + \int_I h_{2s}(\omega_s,\omega_i')\hat{a}_i^\dagger(\omega_i')\,\mathrm{d}\omega_i', \tag{A1a}$$

$$\hat{b}_i(\omega_i)=\int_I h_{1i}(\omega_i,\omega_i')\hat{a}_i(\omega_i')\,\mathrm{d}\omega_i' + \int_S h_{2i}(\omega_i,\omega_s')\hat{a}_s^\dagger(\omega_s')\,\mathrm{d}\omega_s', \tag{A1b}$$

where the output signal (idler) field $\hat{b}_{s(i)}(\omega_{s(i)})$ at frequency $\omega_{s(i)}$ is a superposition of many amplified signal and idler input frequency modes $\hat{a}_s(\omega_s)$ and $\hat{a}_i(\omega_i)$, S and I respectively represent the integration frequency range of the signal and idler fields. In our experiment, the dispersion slope of the DSF is very small and the central wavelength of the pump pulses is in the anomalous-dispersion regime, so we can assume the perfect phase matching condition is always satisfied. In this case, the Green functions h_{1s}, h_{2s}, h_{1i}, h_{2i} can be expressed as[24]

$$h_{1s(i)}(\omega_{s(i)},\omega'_{s(i)})$$
$$=\delta(\omega_{s(i)}-\omega'_{s(i)})+\sum_{n=1}^{\infty}\frac{1}{\sqrt{2n}(2n)!}\frac{G^{2n}}{2\sqrt{\pi}\sigma_p}\mathrm{e}^{\frac{-(\omega_{s(i)}-\omega'_{s(i)})^2}{4\sigma_p^2(2n)}}, \quad (A2a)$$

$$h_{2s(i)}(\omega_{s(i)},\omega'_{i(s)})$$
$$=\sum_{n=0}^{\infty}\frac{1}{\sqrt{2n+1}(2n+1)!}\frac{G^{2n+1}}{2\sqrt{\pi}\sigma_p}\mathrm{e}^{\frac{-(\omega_{s(i)}+\omega'_{i(s)}-2\omega_{p0})^2}{4\sigma_p^2(2n+1)}}, \quad (A2b)$$

where σ_p is the bandwidth of the Gaussian shaped pump and $G\propto\gamma P_p L$ is the gain coefficient of FWM.

After passing through the dual band filter F3 and 50/50 fiber coupler FC2, the signal (idler) field incident on the SPD1 and SPD2 can be written as

$$E_{D1}^{(-)}(t)=E_{D2}^{(-)}(t)$$
$$=\frac{1}{2\sqrt{\pi}}\int \mathrm{d}\omega_{s(i)}f(\omega_{s(i)})\hat{b}_{s(i)}(\omega_{s(i)})\mathrm{e}^{-\mathrm{i}(k_{s(i)}z-\omega_{s(i)}t)}, \quad (A3)$$

where the Gaussian function

$$f(\omega_{s(i)})=\exp\left[-\frac{(\omega_{s(i)}-\omega_{s0(i0)})^2}{2\sigma_{s(i)}^2}\right],$$

with $\sigma_{s(i)}$ denoting the bandwidth is referred to as the spectrum of F3 in signal (idler) band. For simplicity, we assume the quantum efficiency of both SPD1 and SPD2 equal to 1 and ignore the transmission loss because the intensity correlation function is independent of the detection and transmission loss.[22,25] Accordingly, the normalized intensity correlation function measured by the two SPDs is written as

$$g^{(2)}=\frac{\iint \mathrm{d}t_1\,\mathrm{d}t_2\,\langle\alpha|_s\langle 0|_i E_{D1}^-(t_1)E_{D2}^-(t_2)E_{D2}^+(t_2)E_{D1}^+(t_1)|\alpha\rangle_s|0\rangle_i}{\int \mathrm{d}t_1\,\langle\alpha|_s\langle 0|_i E_{D1}^-(t_1)E_{D1}^+(t_1)|\alpha\rangle_s|0\rangle_i\int \mathrm{d}t_2\,\langle\alpha|_s\langle 0|_i E_{D2}^-(t_2)E_{D2}^+(t_2)|\alpha\rangle_s|0\rangle_i}, \quad (A4)$$

where

$$|\alpha\rangle_s=|\{\alpha(\omega_s)\}\rangle=\exp\left\{\int_0^{\infty}[\alpha s(\omega_s)\hat{a}^{\dagger}-\mathrm{h.c.}]\mathrm{d}\omega_s\right\}|0\rangle, \quad (A5)$$

describes the coherent state of the signal input pulses. Here, α is the complex amplitude, and the Gaussian frequency distribution function

$$s(\omega_s)=\frac{1}{\sqrt{\pi^{1/2}\sigma}}\exp\left\{\frac{-(\omega-\omega_{s0})^2}{2\sigma^2}\right\}, \quad (A6)$$

with σ denoting the bandwidth, satisfies the normalization condition $\int_0^{\infty}|s(\omega_s)|^2\mathrm{d}\omega_s=1$. So the photon number of the signal injection is $|\alpha|^2$. The $|0\rangle_i$ in Eq. (A4) describes the vacuum state of the idler input. For detectors with response time much longer than the creation time period of signal and idler photons, which are confined within the pump pulse duration, the time integral can be treated as an integral from $-\infty$ to $+\infty$.

By substituting Eq. (A3) into Eq. (A4), the $g_{s(i)}^{(2)}$ can be calculated and expressed as

$$g_{s(i)}^{(2)}=1+\frac{2H_{s(i)}^{st}+H_{s(i)}^{sp}}{(I_{s(i)}^{st}+I_{s(i)}^{sp})^2}, \quad (A7)$$

where the terms $H_{s(i)}^{st}$, $H_{s(i)}^{sp}$, $I_{s(i)}^{st}$, $I_{s(i)}^{sp}$ are described in detail in the main text.

References

[1] Hansryd J, Andrekson P A, Westlund M, Li J and Hedekvist P O 2002 *IEEE J. Sel. Top. Quant.* **8** 506
[2] Fulconis J, Alibart O, O'Brien J L, Wadsworth W J and Rarity J G 2007 *Phys. Rev. Lett.* **99** 120501
[3] Chen J, Altepeter J B, Medic M, Lee K F, Gokden B, Hadfield R H, Nam S W and Kumar P 2008 *Phys. Rev. Lett.* **100** 133603
[4] Li X Y, Ma X X, Quan L M, Yang L, Cui L and Guo X S 2010 *J. Opt. Soc. Am. B* **27** 1857
[5] Fiorentino M, Voss P L, Sharping J E and Kumar P 2002 *Photon. Technol. Lett.* **14** 983
[6] Fan J, Dogariu A and Wang L J 2005 *Opt. Lett.* **30** 1530
[7] Li X Y, Voss P L, Sharping J E and Kumar P 2005 *Phys. Rev. Lett.* **94** 053601
[8] Li X Y, Yang L, Ma X X, Cui L, Ou Z Y and Yu D Y 2009 *Phys. Rev. A* **79** 033817
[9] Shelby R, Levenson M, Perlmutter S, DeVoe R and Walls D 1986 *Phys. Rev. Lett.* **57** 691
[10] Silberhorn C, Lam P K, Weiß O, König F, Korolkova N and Leuchs G 2001 *Phys. Rev. Lett.* **86** 4267
[11] Sharping J E, Fiorentino M and Kumar P 2001 *Opt. Lett.* **26** 367
[12] Guo X S, Li X Y, Liu N N, Yang L and Ou Z Y 2012 *Appl. Phys. Lett.* **101** 261111
[13] Guo X S, Liu N N, Li X Y, Liu Y H and Ou Z Y 2015 arXiv:1504.07345 [quant-ph]
[14] Peters N A, Toliver P, Chapuran T E, Runser R J, McNown S R, Peterson C G, Rosenberg D, Dallmann N, Hughes R J, McCabe K P, Nordholt J E and Tyagi K T 2009 *New J. Phys.* **11** 045012
[15] Kawahara H, Medhipour A and Inoue K 2011 *Opt. Commun.* **284** 691
[16] Silva N A, Almeida A J and Pinto A N 2012 *Quantum Electron.* **48** 472
[17] Ferreira da Silva T, Xavier G B, Temporão G P and von der Weid J P 2014 *J. Lightwave Technol.* **32** 2332
[18] Ou Z Y 2007 *Multi-photon Quantum Interference* (Berlin: Springer) p. 3
[19] Gerry C and Knight P 2005 *Introductory Quantum Optics* (Cambridge: Cambridge University Press) pp. 4–5
[20] Voss P L, Tang R and Kumar P 2003 *Opt. lett.* **28** 549
[21] Guo X S, Liu N N, Li X Y and Ou Z Y 2015 *Opt. Express* **23** 29369
[22] Ma X X, Li X Y, Cui L, Guo X S and Yang L 2011 *Phys. Rev. A* **84** 023829
[23] Liu N N, Liu Y H, Guo X S, Yang L, Li X Y and Ou Z Y 2016 *Opt. Express* **24** 1096
[24] Guo X S, Li X Y, Liu N N and Ou Z Y 2013 *Phys. Rev. A* **88** 023841
[25] Avenhaus M, Laiho K, Chekhova M V and Silberhorn C 2010 *Phys. Rev. Lett.* **104** 063602